The 11th Canadian Conference on Earthquake Engineering
Canadian Association for Earthquake Engineering

PROBABILISTIC TSUNAMI HAZARD ANALYSIS OF THE CASCADIA SUBDUCTION ZONE AND THE ROLE OF EPISTEMIC UNCERTAINTIES AND ALEATORY VARIABILITY

Hong Kie THIO
AECOM, Los Angeles, United States
hong.kie.thio@aecom.com

Wenwen LI
AECOM, Los Angeles, United States
wenwen.li@aecom.com

ABSTRACT: As part of the process of developing probabilistic tsunami inundation maps for the State of California and the ASCE 7-16 design guidelines, the authors have developed a comprehensive source model for the Cascadia subduction zone and have computed probabilistic offshore exceedance waveheights for different return periods for the entire Cascadia subduction zone. An integral part of the analysis is the formal inclusion of uncertainties, both due to a limited understanding of the physical processes (epistemic) as well their natural variability (aleatory). Since the tsunami inundation process is highly non-linear, it is very important to not only quantify these uncertainties, but also understand how and where to apply them. The tsunami inundation problem can be divided into several stages: the source characterization, deep ocean propagation and nearshore propagation and inundation. In the source characterization, many of the epistemic uncertainties and aleatory variabilities are the same as those specified in probabilistic seismic hazard analysis (PSHA). The biggest difference is in the details of slip distributions, which are very significant in tsunami excitation, especially for near-field tsunamis, but are not used in PSHA. The aithors will show several ways of including slip variability, both stochastic and non-stochastic, which can be used to develop a probabilistic set of source scenarios. The uncertainties in ocean propagation are less significant since modern algorithms are very successful in modeling open ocean tsunami propagation. However, in the near-shore regime and the inundation modeling, the situation is much more complex. Errors in the local elevation models, uncertainty and variability in bottom friction and the omission of built environment are all significant factors that need to be taken into account. Also, even details of the implementation of the tsunami algorithms can yield different results. The most significant sources of uncertainty will discussed and the alternative ways to implement them using examples for the probabilistic tsunami hazard mapping that we are currently carrying out for the state of California and other regions.

1. Introduction

Probabilistic seismic hazard analysis (PSHA) has been a primary tool in the development of design criteria for buildings and infrastructure in engineering for the last few decades. Its use is intricately linked to the use of Performance Based Engineering (PBE) principles, where building design is based on several levels of performance (safe-use, collapse prevention, etc.), which are linked to a particular probability of exceedance of a ground motion level. Risk based analyses also inherently depend on a probabilistic expression of the hazard, and it is thus desirable to follow a similar framework for tsunami hazard analysis (McGuire, 2004). This paper presents an overview of the authors' approach to Probabilistic Tsunami Hazard Analysis (PTHA) applied to the Cascadia subduction zone.

For PTHA, the most obvious metric is the exceedance of a water level, wave amplitude or flow depth, as these are the most visible and recorded aspect of tsunami waves. There are however other metrics that may be more suited for certain purposes, such as flow velocities in ports and harbors or momentum for impact on structures. The current methodology has been developed to compute probabilities of wave height exceedance but can be adapted to analyze other metrics as well.

The probabilities are computed in terms of annual rate of exceedance, which, assuming a Poissonian distribution, can be translated into probability of exceedance in a certain amount of time through:

$$P = 1 - e^{-\gamma t}$$

where *P* is the probability of exceedance in a time period *t* (also called exposure time), and γ the annual rate of exceedance. In engineering applications, we are usually interested in certain probability levels that are expressed in terms of *P*, such as a 2% (.02) probability of exceedance in 50 years, where 50 years is the exposure time *t*. Inverting the above equation as:

$$\gamma = \frac{-\ln(1-P)}{t}$$

the corresponding annual rate of exceedance can then be calculated as .00040405 yr^{-1}, or a recurrence time, often referred to as Average Return Period (ARP), of 2475 yr. Other periods of interest are 10% and 5% in 50 years, which correspond to 475 and 975 years ARP respectively.

In performance based engineering, these probability levels may be tied to a specific performance level, for instance a building may be designed to remain operable for 475 yr ARP level ground motions, be temporarily inoperable but repairable within a reasonable amount of time for the 975 year ground motion levels and not collapse (but be permanently in-operable) for 2475 yr events ("life-safety").

Probabilistic tsunami hazard analysis, like its seismic counterpart, follows a dualistic approach to probability. Whereas some aspects are defined in the familiar terms of frequency of occurrence (such as intermediate earthquake recurrence, magnitude distribution), others are more based on judgment, which is a subjective approach (Vick, 2002). For instance, the recurrence of intermediate earthquakes may be characterized in terms of a Gutenberg-Richter distribution, constrained by a catalog of historical earthquakes. The assumption is that the occurrence of earthquakes is a stationary process, and that the catalog represents a homogenous sample of the long-term seismic behavior of a source. For large earthquakes however, the average return times are often so long relative to our historic record, even when paleo-seismic data is included, that the recurrence properties of these events cannot be described with a stationary model based on a regression of observed earthquake occurrence. We therefore needs to introduce the concept of judgment, where we uses our current understanding of earthquake processes, including analyses of similar structures elsewhere and other information, such as local geological conditions, strain rates etc., to make assumptions on the recurrence of large earthquakes. This is a subjective approach to probability, centered on the observer rather than the observations, and will inevitably be different from one practitioner to the other. A rigorous PTHA model therefore includes the use of logic trees to express alternative understandings of the same process, e.g. large earthquake recurrence, weighted by the subjective likelihood of that alternative model ("degree of belief"), where the weights of the alternatives sum to unity. We shall explain in a later section how this distinction is manifested in the handling of uncertainties throughout the analysis.

1.1. Overview of the AECOM approach

In order to ensure consistency with seismic practice, the AECOM approach closely follows, where possible, the PSHA practice. For instance, the overall framework and inputs remain quite similar to facilitate model exchange between the PSHA and PTHA. There are however some important differences between PSHA and PTHA. The most important difference between the two is the impracticality of using something similar to Ground Motion Prediction Equation (GMPE's, aka Attenuation relations) in tsunami hazard due to the very strong dependence of tsunami waveheights on bathymetry, which precludes the use of simple magnitude distance relations. Fortunately, since the global bathymetry is relatively well

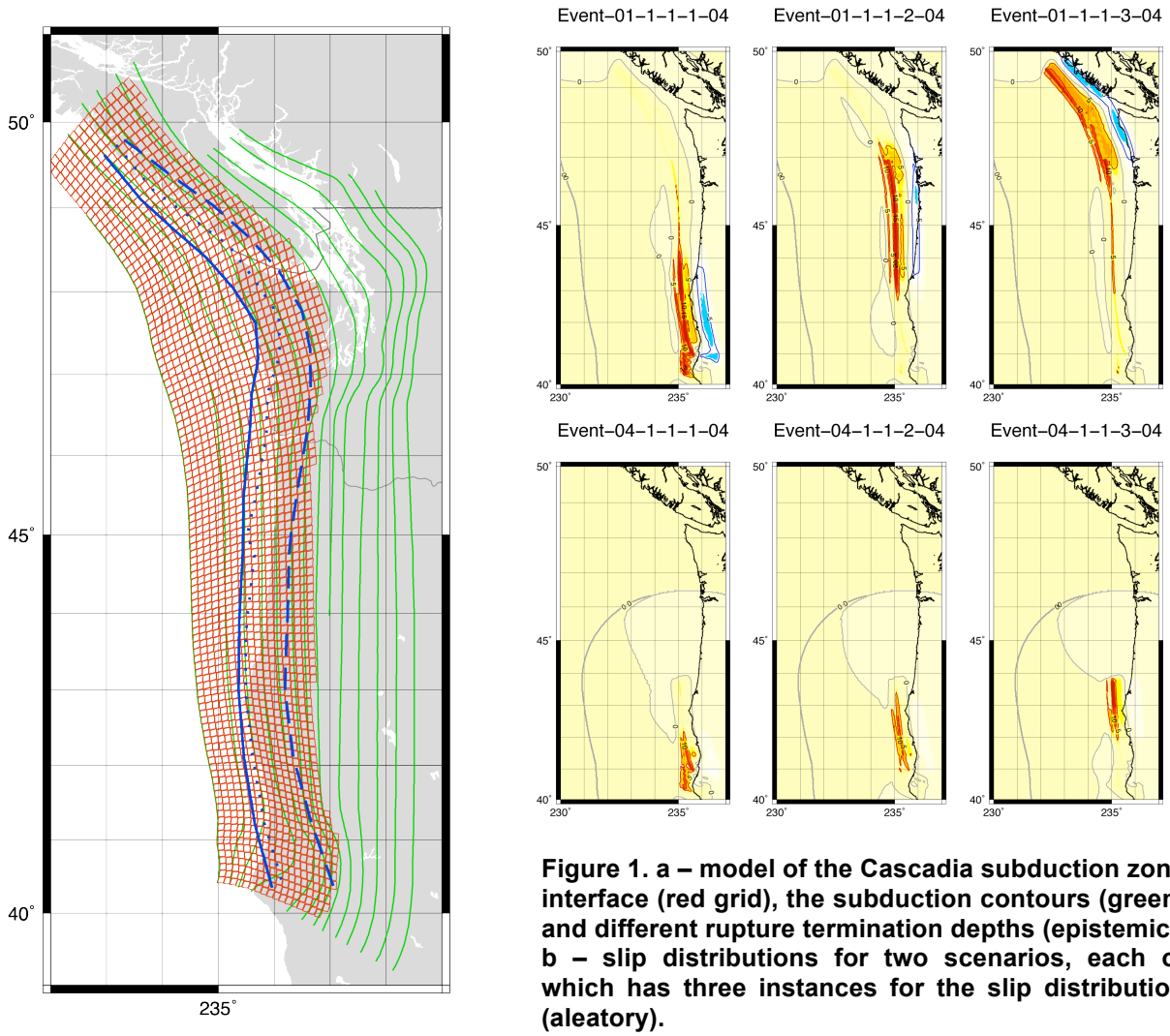

Figure 1. a – model of the Cascadia subduction zone interface (red grid), the subduction contours (green) and different rupture termination depths (epistemic). b – slip distributions for two scenarios, each of which has three instances for the slip distribution (aleatory).

constrained and computational algorithms are sufficiently accurate and efficient, it is possible to replace the GMPE-type relations with actual computed tsunami waveforms. The methodology can be summarized with the following list of steps, with details discussed in later sections:

- Identification and setup (subfault partitioning) of earthquake sources
- Computation of fundamental Green's functions for every sub-fault to near-shore locations
- Definition of earthquake recurrence model
- Generation of a large set of scenario events that represents the full integration over earthquake magnitudes, locations and sources, for every logic tree branch
- Computation of near-shore probabilistic waveheight exceedance rates
- Identification of dominant sources through source dis-aggregation
- Computation of probabilistic inundation hazard by computing non-linear runup using disaggregated sources and offshore waveheights

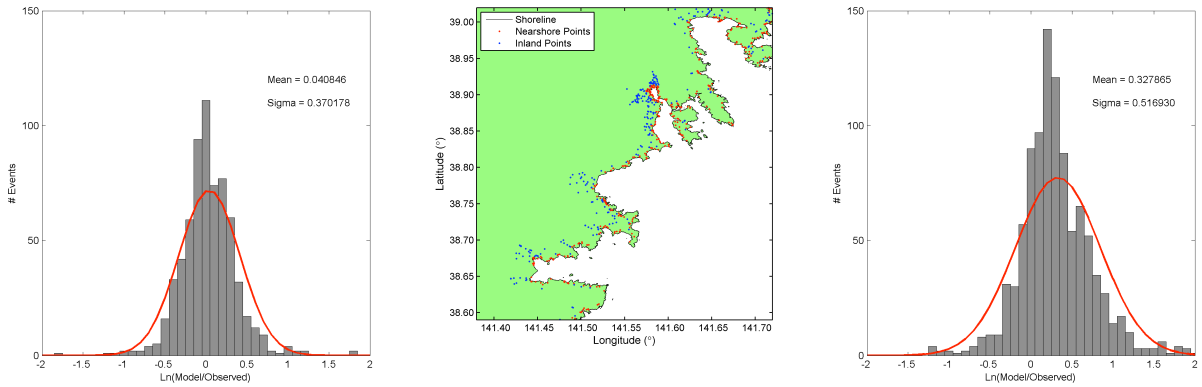

Figure 2. Determination of the modeling uncertainty (aleatory) using the observed flow depths (left graph) and runup (right graph) for the area shown in the center panel.

1.2. Tsunami sources for the Cascadia coast

The procedure for performing a PTHA for Cascadia area (Figure 1) follows along the lines of Thio et al. (2010) but for the inundation part differ because we have to account for both distant and local sources. The offshore probabilistic waveheights contain both the epistemic (alternative source characterizations) and aleatory variability (modeling error, tides, etc.) and as such are fully probabilistic. Disaggregation of the hazard enables us to identify the most significant sources that contribute to the hazard at a particular location for a particular return period. In the case of Cascadia, the dominant sources are the eastern Aleutian subduction zone, the Kuriles and of course the Cascadia subduction zone itself. To achieve the combined hazard from local and distant sources, we start with the hazard curve and source disaggregation for offshore Cascadia. From the disaggregation, we can deduce which of the source zones contribute significantly to the hazard along the shore, and what their relative weights are. For Cascadia, at short return periods the contributions are primarily from Alaska and the Kuriles. As we go to lower probabilities and thus longer return periods, the Cascadia subduction zone becomes rapidly more important and dominates the hazard for return periods larger than 100 -1500 years. The hazard curve gives us the probabilistic hazard levels for different probabilities, and thus gives us as target offshore waveheights for the inundation studies. The procedure for the tele-tsunamis has been developed by Thio et al. (2010).

2. Methodology

Since our approach to PTHA is based on numerical simulations rather than empirical relations, we shall first describe the state of practice in tsunami modeling. This process is usually split into two separate processes: source characterization and tsunami propagation. Tsunami formation results from the deformation of the seafloor, which, in the case of an incompressible liquid and rate of deformation that is much faster than tsunami propagation speed, translates directly in an equivalent vertical disturbance of the sea-surface. It is this disturbance that forms the input condition for the tsunami propagation calculations.

2.1. Source characterization

Earthquake sources are often represented as dislocations on rectangular planes defined by strike and dip. This idealized geometry can deviate significantly from the real situation especially in subduction zones, where the dip tends to increase away from the trench. More recently, curved rupture models have been used and we have adopted such a representation for all our sources using the Slab1.0 (Hayes et al. (2012) model as basis.

2.1.1. Earthquake slip

The tsunami amplitude at the source scales directly with the seafloor uplift, and thus the amount of slip on the rupture plane.

2.1.2. Static deformation

Seafloor uplift due to a dislocation source can be computed using a variety of ways, the most common being Okada's () analytical formulation for displacement resulting from a rectangular dislocation in a half-space. We have used a frequency wavenumber (FK) method for computing displacements as it is more versatile and can accommodate layered crustal structure. In general, elastic models have been shown to be consistent in mapping slip on the fault surface to deformation at the Earth's surface.

For local sources, the near-field uplift and subsidence are incorporated in the final DEM, so that the inundation and runup are consistent with the actual deformation at the surface.

2.2. Tsunami models

Because of their long wavelengths (100's of kilometers), relative to the depth of the oceans (up to 10 km), we can use the long wave approximation to the governing equations of water waves, the Navier-Stokes and continuity equations. There are several approximations made the solution of this equation, the most restrictive being the linear shallow water equations.

2.2.1. Formulation

For tsunami simulations these equations are typically solved in two dimensions, with vertical accelerations either ignored completely (shallow water or hydrostatic approximation) or approximated in Bousinesq-type models. The simplest (and computationally fastest) form uses the linear shallow water equations. These are generally adequate for tsunami modeling on open oceans but not for near-shore environments as they don't include bottom friction or inundation. Non-linear shallow water equations are suitable for nearshore and inundation studies.

2.2.2. Numerical aspects

The equations of motion can be solved using different methods, the most common being finite difference (e,g, COMCOT, TUNAMI, MOST) although finite volume methods (e.g. ANUGA, GeoClaw, FUNWAVE) are also popular due to the ease of preserving mass and momentum, a potentially important issue in the case of steep gradients such as bore formation.

2.2.3. Bottom friction

For nearshore and runup modeling, bottom friction is an important parameter. This dissipative term can be included in different ways, the most common being a dimensionless friction parameter and the Manning's coefficient. In our calculations, a Manning's coefficient of .025 was used uniformly throughout the computational domain.

2.3. Bathymetric models

Accurate bathymetric and topographic models are essential for tsunami hazard studies. For open ocean modeling, global models such GEBCO or ETOPO1 provide sufficient accuracy, but in near-shore regions these are often insufficient, bith in term of accuracy as well as horizontal resolution.

Likewise, the global topographic models such SRTM and ASTER are not accurate enough for inundation modeling. The errors are one the order of 10-15 meters and especially in the case of SRTM, there appears to be a systematic bias to higher elevations in coastal areas (Figure).

3. Probabilistic hazard analysis

Probabilistic hazard analysis is often used in engineering design, planning, and risk analysis. It is desirable to frame tsunami hazard analysis into a probabilistic manner, in a manner that is consistent with other hazards such as seismic hazard, not only in concept, but also in a consistent use of the underlying physical models such as earthquake sources.

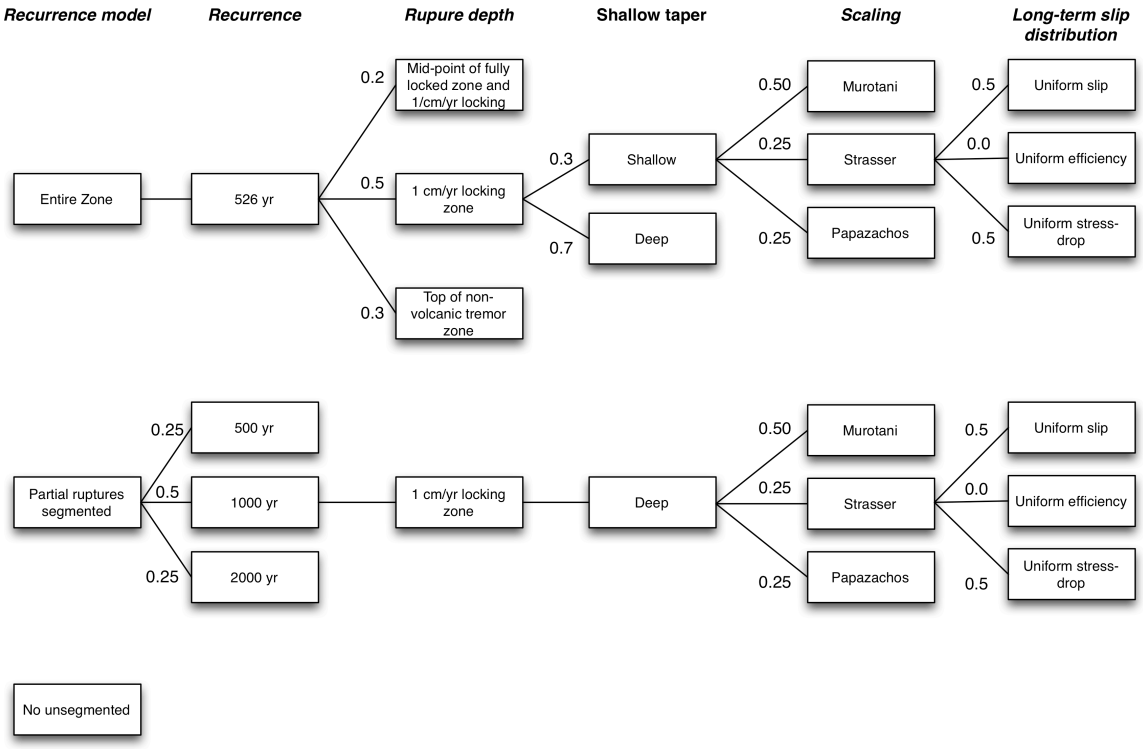

Figure 3. Logic tree model for the Cascadia subduction zone, based on the model used for the 2014 US National Seismic Hazard Maps

3.1. Epistemic uncertainty

Frankel (pers. comm., 2012) developed a set of six different rupture extents along the Cascadia subduction zone with associated average return periods based on the aforementioned work of Goldfinger et al. (2011) and other studies. These scenarios are shown in Table 1. These ruptures, which are only defined in terms of length segments along the Cascadia zone form the basis of our source model, are further defined in a logic tree framework that addresses the epistemic uncertainties in fault width, splay faulting as well as aleatory uncertainties such as slip variability.

3.1.1. Up dip rupture termination and splay faulting

It is often assumed that the shallow part of a subduction zone cannot support large differential stresses and that earthquakes cannot nucleate here (e.g. Scholz, 1998), but can penetrate at least partially into it. Lay et al. (2012) concluded , on the basis of observed tsunamigenic earthquakes that this zone can deform aseismically but can also sustain large earthquakes but with a slower rupture velocities and thus longer durations compared to deeper events. Therefore, in our model three alternative branches are included that allow no slip, 75% and 50% of the deeper slip to occur in the shallow zone (Table 2). In the latter two models, the remainder of the slip is accommodated on splay faulting.

Significant movement along splay faults have been observed or inferred in several large subduction zones, the most unambiguous and prominent case being the movement along the Patton Bay Fault during the 1964 Alaska earthquake (Plafker 1965).

The Cascadia subduction zone features a well-defined zone of splay faulting that is visible on-land in the Humboldt Bay area and has been mapped offshore along most of the Cascadia coast. It is therefore likely that this feature will be active during a large interface earthquake.

3.1.2. Down dip rupture termination

Although slip at the deepest part of the rupture may not contribute directly to the tsunami generation, it is still very important for the following reasons:

The uplift and subsidence of the coast-line are strongly dependent on the location of the rupture termination

Since the magnitude and slip are tied to the rupture area through scaling relations, a larger width of the fault will increase the average slip on the fault.

The down dip termination has been studied extensively (e.g. Wang et al., 2003) and there is general agreement on the fact that the Cascadia rupture is quite narrow (< 50 km) compared to other major subduction zone systems.

This geometry is quite similar to the one used by Witter et al. (2011).

3.2. Aleatory variability

3.2.1. Magnitude/average slip

The rupture length (from the base models) and rupture width (from the logic tree) provide us with an area (*A*) which through the published scaling relations, which in the case of Strasser et al. (2010) is:

$$M = 4.441 + 0.841 * \log(A), \sigma = 0.286$$

gives us magnitude (*M*), and thus earthquake moment (M_0 – in Nm):

$$M_W = \frac{\log(M_W) - 9.1}{1.5}$$

The average slip is (*D*) then obtained through:

$$D = \frac{M_0}{\mu A}$$

We sample the magnitude area distribution at five points from -2 to +2 sigma.

3.2.2. Variable slip

In previous analyses (e.g. Thio et al., 2010), we have used uniform slip models to produce tsunami waves. At local distances however, the slip variability becomes an important factor and asperities with large amounts of slip can cause significantly higher tsunami waves, especially locally, as is illustrated by the recent Tohoku earthquake where the maximum slip exceeded the average slip by at least a factor of 2.

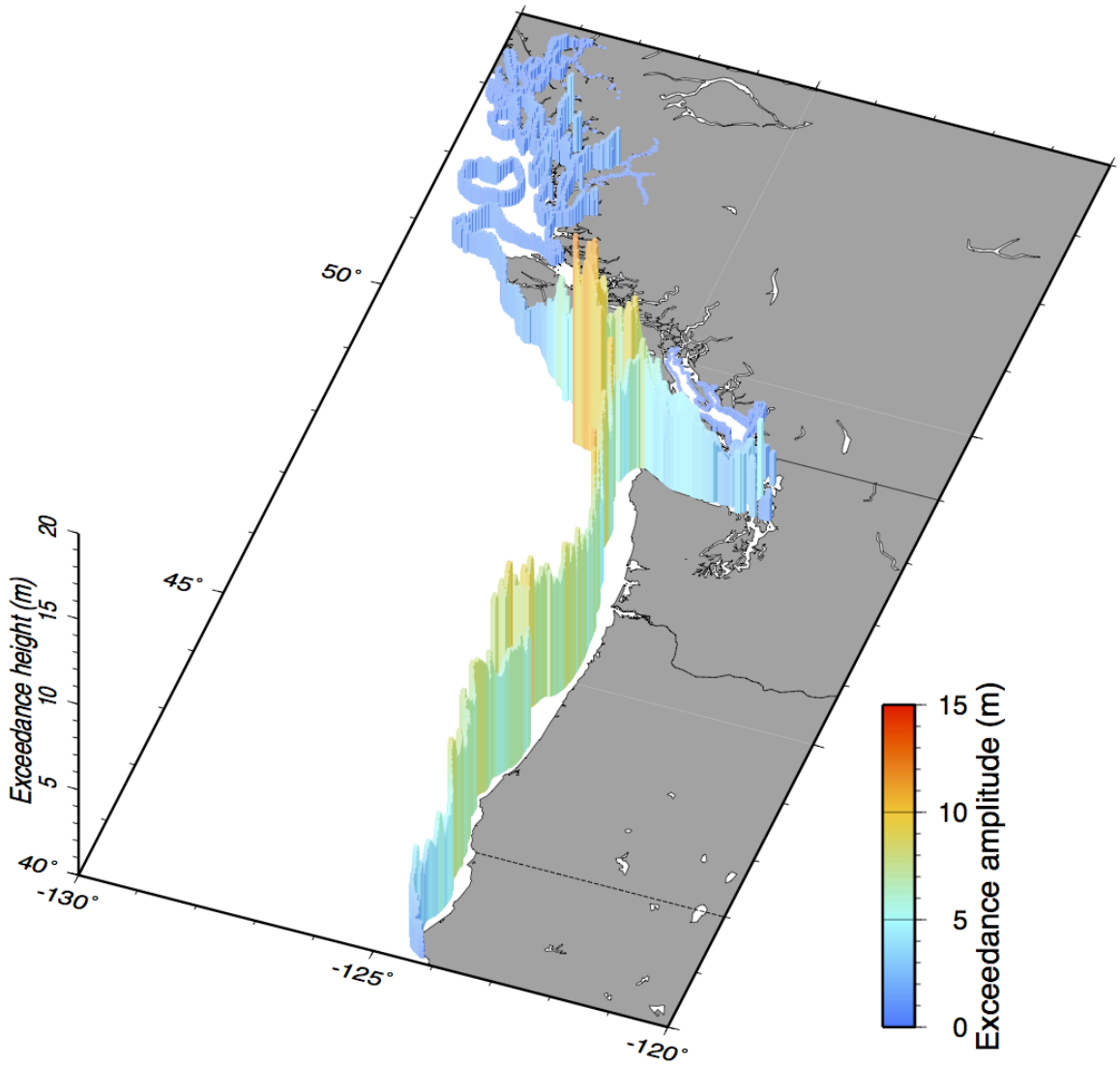

Figure 4. Probabilistic offshore exceedance amplitudes for a return period of 2500 years, based on Cascadia sources.

Murotani et al. (2008) studied the slip distributions of several subduction zone earthquakes and found a ratio of maximum slip over average slip of 2.2. To include this slip variability, we used variable slip rupture models with on third of the rupture as an asperity with twice the average slip and the other two-thirds of the rupture at half the average slip. We computed a total of three scenarios (Figure 1) for each event where the asperity occupies every part of the rupture once. This way, there is no risk that in some areas the hazard is over- or under-estimated due to incomplete or overlapping asperity coverage offshore.

3.2.3. Tidal variability

The tidal variability is included in the offshore waveheights for the tele-tsunami sources by convolving the time-series with a local tidal record. This ensures that in the case of multiple high waves, the probability of coinciding with a high tide is properly taken into account. For the Cascadia source, our original intent was to compute scenarios at a number of tide levels, and weigh them according to a similar distribution function. However, that would increase the number of run dramatically and we decided instead to include

the tidal component for the local runs in the same way as the aleatory uncertainty for the inundation, i.e. after the inundation has been computed.

3.2.4. Tsunami modeling uncertainty

Thio et al. (2010) included a sigma term for the modeling uncertainty based on the analysis of observed and modeled tsunami waveheights for several well-constrained tsunamis along the west coast. These uncertainties only cover the oceanic propagation to the shoreline since most data were obtained from tide gage records. For the aleatory uncertainty in the inundation and runup from a local earthquake we need to establish a new term, which requires detailed modeling of runup data from a well-constrained event. The recent Tohoku earthquake provides a wealth of data for this purpose (Figure 2), but we have not modeled this event in detail yet. The Okushiri benchmarking exercise does provide data that can be used for this purpose as well, and in Figure 10 we show the comparison of our model and the data. If we simply compare the average values and perform a regression over the ratio ln(data)/ln(model) we obtain a standard deviation of 0.36 (Figure 10) and only a small bias (.04). In contrast to the previous aleatory terms, we apply this uncertainty to the inundation waveheights, i.e. after the modeling, because that is how the sigma was determined. A drawback to this is that although the modeling uncertainty is incorporated in a consistent way, it will not automatically extend the inundation line since the sigma will not have an effect on areas with zero waveheight.

4. Results

In Figure 4, the results of the probabilistic offshore hazard analysis for Cascadia are shown (at the 100 m depth contour) for a return period of 2500 year (2% in 50 yr exceedance). The hazard is obviously very high for the coast that is directly exposed to the megathrust, whereas outside the area the exceedance amplitudes drop off substantially and rapidly. This is consistent with observations in previous megathrust environments worldwide. These results can be used in different ways. For large scale risk mapping analyses, it may be sufficient to project these offshore amplitudes on-land using empirical runup relationships. For more accurate inundation and runup studies, the offshore waveheghts can be used to constrain detailed runup calculations, a process that is currently being followed for the creation of the inundation hazard maps for the State of California as well as ASCE-7-16.

5. References

Earthquake Research Committee, 2005, National seismic hazard maps for Japan, Headquartes of Earthquake Research Promotion, Japan.

Fluck, P., Hyndman, R., and Wang, K., 1997, Three-dimensional dislocation model for great earthquakes of the Cascadia subduction zone: Journal of Geophysical Research, v. 102, no. B9, p. 20539–20–550.

Goldfinger, C., Kulm, L.V.D., McNeill, L.C., and Watts, P., 2000, Super-scale failure of the southern Oregon Cascadia margin: Pure and Applied Geophysics, v. 157, no. 6-8, p. 1189–1226.

Goldfinger, C., Nelson, C.H., Morey, A., Johnson, J.E., Gutierrez-Pastor, J., Eriksson, A.T., Karabanov, E., Patton, J., Gracia, E., and Enkin, R., 2011, Turbidite Event History: Methods and Implications for Holocene Paleoseismicity of the Cascadia Subduction Zone, USGS Professional Paper 1661-F, Reston, VA: US Geological Survey, v. 332.

Hayes, G. P., D. J. Wald, and R. L. Johnson (2012), Slab1.0: A three-dimensional model of global subduction zone geometries, J. Geophys. Res., 117, B01302, doi:10.1029/2011JB008524.

Hawkes, A.D., Horton, B.P., Nelson, A.R., Vane, C.H., and Sawai, Y., 2011, Coastal subsidence in Oregon, USA, during the giant Cascadia earthquake of AD 1700: Quaternary Science Reviews, v. 30, no. 3-4, p. 364–376, doi: 10.1016/j.quascirev.2010.11.017.

Heaton, T.H., and Kanamori, H., 1984, Seismic potential associated with subduction in the northwestern United States: Bulletin of the Seismological Society of America, v. 74, no. 3, p. 933–941.

Jacoby, G.C., Bunker, D.E., and Benson, B.E., 1997, Tree-ring evidence for an AD 1700 Cascadia

earthquake in Washington and northern Oregon: Geology, v. 25, no. 11, p. 999–1002.

Lay, T., Kanamori, H., Ammon, C.J., Koper, K.D., Hutko, A.R., Ye, L., Yue, H., and Rushing, T.M., 2012, Depth-varying rupture properties of subduction zone megathrust faults: Journal of Geophysical Research, v. 117, no. B4, doi: 10.1029/2011JB009133.

Leonard, L.J., Currie, C.A., Mazzotti, S., and Hyndman, R.D., 2010, Rupture area and displacement of past Cascadia great earthquakes from coastal coseismic subsidence: Geological Society of America Bulletin, v. 122, no. 11-12, p. 2079–2096, doi: 10.1130/B30108.1.

Ludwin, R.S., Dennis, R., Carver, D., McMillan, A.D., Losey, R., Clague, J., Jonientz-Trisler, C., Bowechop, J., Wray, J., and James, K., 2005, Dating the 1700 Cascadia earthquake: great coastal earthquakes in Native stories: Seismological Research Letters, v. 76, no. 2, p. 140–148.

Mazzotti, S., 2003, Current tectonics of northern Cascadia from a decade of GPS measurements: Journal of Geophysical Research, v. 108, no. B12, p. 2554, doi: 10.1029/2003JB002653.

McCrory, P.A., Blair, J.L., Oppenheimer, D.H., and Walter, S.R., 2006, Depth to the Juan de Fuca slab beneath the Cascadia subduction margin: A 3-D model for sorting earthquakes, Data Ser. 91: US Geol. Surv., Reston, Va.

Murotani, S., Miyake, H., and Koketsu, K., 2008, Scaling of characterized slip models for plate-boundary earthquakes: Earth, Planets and Space, v. 60, no. 9, p. 987.

Nelson, A.R., Atwater, B.F., Bobrowsky, P.T., Bradley, L.-A., Clague, J.J., Carver, G.A., Darienzo, M.E., Grant, W.C., Krueger, H.W., and Sparks, R., 1995, Radiocarbon evidence for extensive plate-boundary rupture about 300 years ago at the Cascadia subduction zone:.

Nelson, A.R., Kelsey, H.M., and Witter, R.C., 2006, Great earthquakes of variable magnitude at the Cascadia subduction zone: Quaternary Research, v. 65, no. 3, p. 354–365, doi: 10.1016/j.yqres.2006.02.009.

Shaw, B.E., and Wesnousky, S.G., 2008, Slip-Length Scaling in Large Earthquakes: The Role of Deep-Penetrating Slip below the Seismogenic Layer: Bulletin of the Seismological Society of America, v. 98, no. 4, p. 1633–1641, doi: 10.1785/0120070191.

Strasser, F.O., Arango, M.C., and Bommer, J.J., 2010, Scaling of the Source Dimensions of Interface and Intraslab Subduction-zone Earthquakes with Moment Magnitude: Seismological Research Letters, v. 81, no. 6, p. 941–950, doi: 10.1785/gssrl.81.6.941.

Thio, H.K., Somerville, P.G., and Polet, J., 2010, Probabilistic tsunami hazard in California: Pacific Earthquake Engineering Research Center Report, v. 108, p. 331.

Wang, K., 2003, A revised dislocation model of interseismic deformation of the Cascadia subduction zone: Journal of Geophysical Research, v. 108, no. B1, p. 2026, doi: 10.1029/2001JB001227.

Wesson, R.L., 2007, Revision of time-independent probabilistic seismic hazard maps for Alaska, USGS OFR-2007-1043.

Witter, R.C., Zhang, Y., Wang, K., Priest, G.R., Goldfinger, C., Stimely, L.L., English, J.T., and Ferro, P.A., 2011, Simulating tsunami inundation at Bandon, Coos County, Oregon, using hypothetical Cascadia and Alaska earthquake scenarios: Special Paper Oregon Department of Geology and Mineral Industries.